Micro and Nano Systems Letters

LETTER

Open Access

Synthesis of metallic aluminum particles by electrolysis in aqueous solution

Takefumi Hosoya[1], Takehiro Yonezawa[2], Noriko Yamauchi[1], Kouichi Nakashima[1*] and Yoshio Kobayashi[1*]

Abstract

The present work proposes a method for fabricating metallic Al particles in aqueous solution. An aqueous colloidal solution was prepared from an aqueous aluminum nitrate nonahydrate solution by electrolysis using metallic Al plates as the anode and cathode under ultrasonic irradiation in water at 25–45 °C. The sizes of the particles in the colloidal solutions prepared at 25, 35, and 45 °C were 76.3, 77.0, and 84.7 nm, respectively. The powder obtained from the colloidal solution prepared at 25 °C was not crystalline. By contrast, the powders obtained from the colloidal solutions prepared at 35 and 45 °C had a crystal structure of cubic Al and crystal sizes of 55.7 and 59.3 nm, respectively. Thus, elevated temperatures promoted both particle growth and crystal growth, which was explained by higher temperatures increasing the frequency and energy of particle collisions. The metallic Al particles were chemically stable in both an aqueous solution and the ambient atmosphere. The chemically stable metallic Al particles are expected to be used as sources for fabricating materials related to fuels, energy storage, and pigments.

Keywords: Aluminum, Particle, Aqueous colloidal solution, Electrolysis

Introduction

Nanoparticles and microparticles of metallic materials are widely known to exhibit properties that differ from those of the corresponding bulk materials. Hence, metallic particles are used in fields related to catalysis, optics, and biotechnology [1–3]. Metallic Al particles have also been investigated for potential applications as fuels, energy storage materials, and pigments [4–6]. Many reported methods for synthesizing metallic Al particles involve the electrical evaporation or explosion of metallic Al wire in a gaseous medium, which is a well-known gas-phase process for synthesizing particles [7–12]. Although this gas-phase process works well, it requires equipment that is expensive, consumes a large amount of electric power, and is complicated and dangerous to perform.

An alternative method to produce metallic particles is liquid-phase reactions. Most such reactions involve the reduction of metal ions in an aqueous phase. This process can easily produce a large amount of metallic particles and is therefore suitable for industrial production. Particles of noble metals such as Au, Pt, and Ag can be synthesized via the reduction of metal ions in aqueous solution [13–15]. However, the synthesis of less-noble metals in aqueous solution is difficult. For example, the corrosion of metallic Al in aqueous electrolytes leads to oxidation of metallic Al by the reaction $2Al + 6H_2O \rightarrow 2Al(OH)_3 + 3H_2\uparrow$ [16], which makes both the synthesis and long-term storage of metallic Al particles difficult. Metallic Al particles can be synthesized via a process based on the reduction of Al^{3+} ions in organic solvents [17, 18]. The organic solvents are used to inhibit the oxidation derived from aqueous electrolytes. However, the use of organic solvents increases the environmental impact.

Typical methods for producing metals and metal alloys are electrolytic processing (electrolysis) techniques such as electrodeposition and electroplating [19–23]. The

*Correspondence: kouichi.nakashima.pilot@vc.ibaraki.ac.jp; yoshio.kobayashi.yk@vc.ibaraki.ac.jp
[1] Department of Materials Science and Engineering, Graduate School of Science and Engineering, Ibaraki University, 4-12-1 Naka-narusawa-cho, Hitachi, Ibaraki 316-8511, Japan
Full list of author information is available at the end of the article

electrolytic deposition of metallic Al has been reported [24–26]. The electrolysis process does not usually involve reducing reagents and therefore can increase the purity of the metal. Electrolysis usually forms a metallic film on the electrode via the deposition of metal nanoparticles. If the metallic particles deposited onto the electrode can be dispersed in the electrolyte, the dispersion can yield a colloidal solution of metallic particles. From this viewpoint, several researchers have synthesized metallic particles using electrolysis [27–29]. Methods for the electrolytic synthesis of metallic Al particles, in particular, have also been reported [30–32]. In these methods, an organic solvent, ionic liquid, and strong reducing reagent are used, which creates a large environmental load, introduces high costs, poses a danger to human health and the environment, and leads to adulteration of the product by impurities that originate from the reducing reagent. Unsurprisingly, the synthesis of metallic Zn particles in water is also challenging. Nevertheless, our research group has synthesized metallic Zn particles via electrolysis in aqueous solution.

In the present study, we extend our method used to prepare metallic-Zn-particle colloidal solutions in water by electrolysis to prepare high-purity metallic Al particles via a simple method with low environmental impact, which is also challenging.

Experimental

Materials

Aluminum nitrate nonahydrate ($Al(NO_3)_3{\cdot}9H_2O$) (98.0%, Kanto Chemical Co.) was used as received as the starting reagent for preparing metallic Al particle colloidal solutions. Metallic Al plates with dimensions of $20 \times 75 \times 0.5$ mm^3 were used as the electrodes. A commercial metallic Al plate (purity: 99.7%, dimensions: $45 \times 120 \times 0.5$ mm^3, code #: 1–126-0119, Kenis) was divided into metallic Al plates with the desired size. All the aqueous solutions were prepared using water purified by ion exchange and distillation with an Advantec RFD372NC water distillation apparatus.

Preparation

Figure 1 shows an illustration of set-up of fabrication of metallic Al nanoparticles by electrolysis in aqueous solution. The electrolytic solution was a 0.1 M $Al(NO_3)_3$ aqueous solution prepared using purified water, in which the oxygen was removed by N_2 bubbling. One hundred milliliters of the electrolyte solution was placed in a beaker with a capacity of 100 mL. Electrolysis was carried out at room temperature using a two-electrode system with a constant current in the electrolytic solution. The Al plates were used as both the anode and the cathode. At the anode, Al^{3+} should be supplied to the electrolyte solution, as represented by the reaction $Al \rightarrow Al^{3+} + 3e^-$. At the cathode, the reaction $Al^{3+} + 3e^- \rightarrow Al$ should occur, where Al^{3+} is supplied from the reagent used to prepare the electrolyte and by the reaction $Al \rightarrow Al^{3+} + 3e^-$ at the anode. Metallic Al should be produced through deposition of Al nuclei followed by growth of the nuclei into Al nanoparticles on the cathode. The two electrodes were submerged in 2 cm of the electrolytic solution such that the distance between them was 2 cm. The voltage was applied using an A&D AD-8724D DC stabilized power supply to maintain a current constant of 1.0 A. The electrolysis time was 60 min. To disperse the Al nanoparticles deposited onto the cathode into the electrolytic solution prior to the formation of metallic bulk Al, the bottom of the beaker was irradiated with ultrasonic waves generated by a Honda Electronics W-113 ultrasonic cleaner (oscillation frequency: 28 kHz) during electrolysis.

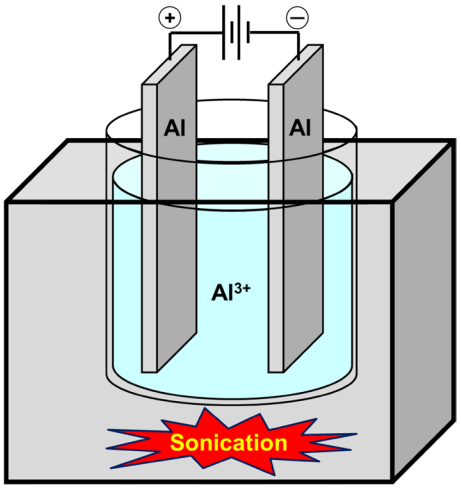

Fig. 1 Illustration of set-up of fabrication of metallic Al nanoparticles by electrolysis in aqueous solution

Characterization

The morphology and crystal structure of the particles were investigated by transmission electron microscopy (TEM) and X-ray diffraction (XRD), respectively. TEM imaging was performed using a JEOL JEM-2100 microscope operating at 200 kV. The TEM samples were prepared by dropping the colloidal solution onto a collodion-coated Cu grid and evaporating its dispersant. The volume-averaged particle size and the standard deviation of the particle size distribution were determined using dozens of particle diameters measured in the TEM images. The XRD measurements were carried out using a Rigaku Ultima IV X-ray diffractometer with a CuKα radiation source operated at 40 kV and 30 mA.

The XRD samples were powders of the particles. The particles in the colloidal solution were washed by repeated centrifugation and decantation to remove the supernatant, followed by the addition of water and redispersion by shaking using a vortex mixer. The washing process was performed three times, and the particle powder was obtained by centrifuging the colloidal solution, removing its supernatant by decantation in the third washing process, and drying the slightly wet particle powder in a Yamato DP-31 vacuum drying oven equipped with an oil-sealed rotary vacuum pump (ULVAC GCD-136X).

Results and discussion

Electrolysis at room temperature (25 °C)

Figure 2a shows a photograph of the electrolytic solution before electrolysis. The solution was transparent at this point. Figure 2b shows a photograph of the electrolytic solution prepared by electrolysis at 25 °C. The transparent electrolytic solution became a slightly opaque and grayish colloid solution after electrolysis. No significant precipitation occurred after a few hours of preparation, as far as the naked eye could determine. The solution could therefore be regarded as colloidally stable. The opaqueness implied the production of nanoparticles that caused light scattering.

Figure 3a shows a TEM image of particles contained in the colloidal solution. Several particles were observed, and their size was 76.3 ± 30.2 nm. Pattern (a) in Fig. 4 shows the XRD pattern of the particles obtained at room temperature. No remarkable peaks were detected, which indicates that the particles were either amorphous or crystallites that were too fine to be detected.

Electrolysis under heating

Figure 2c, d show photographs of the electrolytic solutions prepared after the electrolysis at 35 and 45 °C, respectively. Like the product obtained at 25 °C, those obtained at 35 and 45 °C were slightly opaque, grayish, and colloidally stable solutions. Figure 3b, c show TEM images of particles in the colloid solutions. The particle sizes were 77.0 ± 31.0 nm for product obtained at 35 °C and 84.7 ± 38.2 nm for those obtained at 45 °C. Thus, the particle size increased with increasing temperature of the electrolytic solution. The particles collided with greater

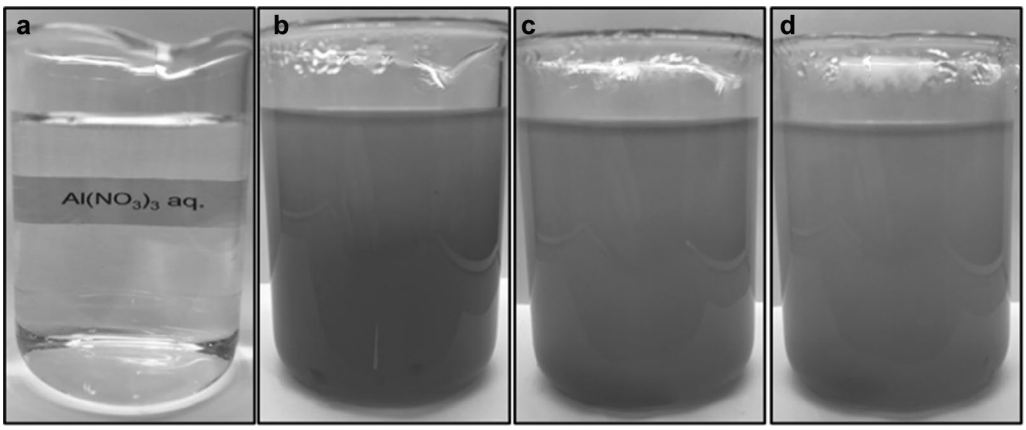

Fig. 2 Photographs of **a** $Al(NO_3)_3$ aqueous solution and colloidal solutions prepared by electrolysis at **b** 25 °C, **c** 35 °C, and **d** 45 °C

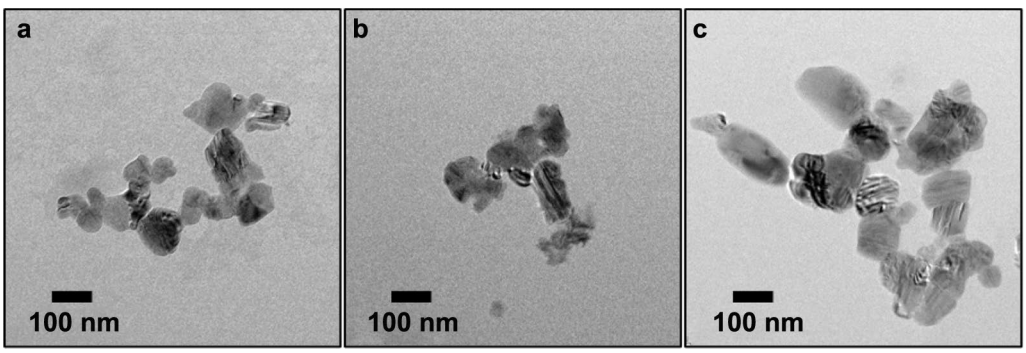

Fig. 3 TEM images of nanoparticles in colloidal solutions prepared by electrolysis at **a** 25 °C, **b** 35 °C, and **c** 45 °C

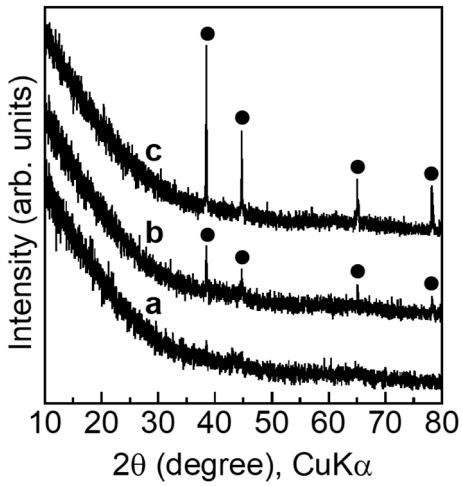

Fig. 4 XRD patterns for nanoparticles in colloidal solutions prepared by electrolysis at **a** 25 °C, **b** 35 °C, and **c** 45 °C. ●: cubic Al

energy at higher temperatures, which resulted in aggregation of the nanoparticles and an increase of the average particle size.

Figure 4 shows the XRD results. Profile (b) is for particles produced at 35 °C. Peaks were detected at 38.5°, 44.7°, 65.1°, and 78.2°. These peaks were assigned to the (111), (200), (220), and (311) planes of metallic Al (cubic), respectively, according to previously published results [26, 33] and an ICDD reference pattern (#00-004-0787). These peak assignments confirmed the production of metallic Al particles. An increase in temperature during electrolysis was considered to promote reduction of Al^{3+} ions and crystallization of particles. By applying the Scherrer equation to the XRD linewidth for the (111) plane peak, we determined that the average metallic Al crystal size was 55.7 nm. The observed particle size is larger than the crystal size determined by XRD analysis, although they are similar. This result suggests that the metallic Al particles were a mixture of single crystals and polycrystals of metallic Al. However, the formation of a single crystals cannot be confirmed from XRD powder diffraction analysis alone, and analyses using other analytical techniques, such as electron-backscatter diffractometry and selected-area electron diffractometry, are required to demonstrate the formation of a single crystal.

Profile (c) in Fig. 4 is for nanoparticles produced at 45 °C. Peaks assigned to the (111), (200), (220), and (311) planes of metallic Al (cubic) appeared at 38.5°, 44.7°, 65.1°, and 78.2°, respectively. The average Al crystal size was 59.3 nm; in this case also, the particle size was larger than the crystal size but the sizes were similar. The metallic Al nanoparticles were similarly speculated to be a mixture of single crystals and polycrystals of metallic Al.

The crystal size increased from 55.7 to 59.3 nm when the temperature was increased from 35 to 45 °C. This temperature dependence of the particle size reconfirms that higher temperatures promote the crystallization of particles. Notably, no peaks attributable to phases other than metallic Al (e.g., Al oxide) were observed in the XRD profiles for the products obtained at either temperature. According to Rai et al. [34], oxidation of metallic Al occurs via the diffusion of oxygen. Such oxidation was not observed in the present work, which indicates that the obtained metallic Al particles were chemically stable, although the mechanism for this high chemical stability remains unclear.

Gas evolution

Bubbles were generated on the anode in all the electrolysis experiments. The reaction $2H_2O \rightarrow O_2 + 4H^+ + 4e^-$, which results in gas evolution, must have occurred because the electrolyte solutions contained no substances prone to oxidation other than water. The standard potential of the reaction $O_2 + 4H^+ + 4e^- \rightleftharpoons 2H_2O$ is +1.229 V [35]; thus, the reaction $2H_2O \rightarrow O_2 + 4H^+ + 4e^-$ does not progress easily. Because electrons in the anode moved toward the power supply via current flow, electrons were depleted at the anode. Therefore, the reaction $2H_2O \rightarrow O_2 + 4H^+ + 4e^-$ progressed to the right, which led to O_2 evolution at the anode. Thus, the bubbles were regarded as O_2 gas produced by the oxidation of water. Because the current flow was provided by electrons generated by both the reactions $2H_2O \rightarrow O_2 + 4H^+ + 4e^-$ and $Al \rightarrow Al^{3+} + 3e^-$ at the anode, the O_2 evolution that resulted from the reaction $2H_2O \rightarrow O_2 + 4H^+ + 4e^-$ would have disturbed the reaction $Al \rightarrow Al^{3+} + 3e^-$ at the anode. Thus, O_2 evolution may have reduced the efficiency of the production of metallic Al particles because this disturbance did not supply Al^{3+} ions to the electrolyte solution. The development of a highly efficient method for synthesizing metallic Al particles is a challenge and will be addressed in future work.

Conclusions

A method for fabricating metallic Al particles in aqueous solution was proposed. An aqueous colloidal solution of metallic Al nanoparticles with a cubic crystal structure was prepared by reducing Al^{3+} ions via electrolysis onto metallic Al-plate electrodes under ultrasonic irradiation and heating. The particle sizes were 76.3 nm at 25 °C, 77.0 nm at 35 °C, and 84.7 nm at 45 °C, and the crystal sizes were 55.7 nm at 35 °C and 59.3 nm at 45 °C. Higher temperatures led to greater collisions among the nanoparticles, which promoted particle growth followed by crystal growth. The metallic Al particles were chemically stable not only in aqueous solution but also in air.

In conclusion, we demonstrated that chemically stable and colloidally stable metallic Al particles can be synthesized via electrolysis in water. Our future challenge is to develop a highly efficient synthesis method.

Abbreviations
TEM: Transmission electron microscopy; XRD: X-ray diffraction.

Acknowledgements
The authors are indebted to Mr. S. Furukawa, who energetically analyzed the measurement results.

Authors' contributions
TH synthesized the samples, performed all the characterizations, and drafted the manuscript, under TY, NY, KN, and YK's supervision. TY, NY, KN, and YK modified and finished the manuscript. All authors read and approved the final manuscript.

Funding
No funding was received.

Availability of data and materials
The datasets supporting the conclusions of this article are included within the article.

Declarations

Ethics approval and consent to participate
Not applicable.

Consent for publication
Not applicable.

Competing interests
The authors declare that they have no competing interests.

Author details
[1]Department of Materials Science and Engineering, Graduate School of Science and Engineering, Ibaraki University, 4-12-1 Naka-narusawa-cho, Hitachi, Ibaraki 316-8511, Japan. [2]Central Research Institute, Mitsubishi Materials Corporation, 1002-14 Mukohyama, Naka, Ibaraki 311-0102, Japan.

Received: 19 April 2021 Accepted: 2 December 2021
Published online: 08 December 2021

References

1. Serra-Maia R, Chastka S, Bellier M, Douglas T, Rimstidt JD, Michel FM (2019) Effect of particle size on catalytic decomposition of hydrogen peroxide by platinum nanocatalysts. J Catal 373:58–66
2. Sharma P, Semwal V, Gupta BD (2019) A highly selective LSPR biosensor for the detection of taurine realized on optical fiber substrate and gold nanoparticles. Opt Fiber Technol 52:101962
3. Munir T, Mahmood A, Imran M, Sohail A, Fakhar-e-Alam M, Sharif M, Masood T, Bajwa SZ, Shafiq F, Latif S (2021) Quantitative analysis of glucose by using (PVP and MA) capped silver nanoparticles for biosensing applications. Phys B 602:412564
4. Pourmortazavi SM, Hajimirsadeghi SS, Kohsari I, Fathollahi M, Hosseini SG (2008) Thermal decomposition of pyrotechnic mixtures containing either aluminum or magnesium powder as fuel. Fuel 87:244–251
5. Bunker CE, Smith MJ, Fernando KAS, Harruff BA, Lewis WK, Gord JR, Guliants EA, Phelps DK (2010) Spontaneous hydrogen generation from organic-capped Al nanoparticles and water. ACS Appl Mater Interfaces 2:11–14
6. Karlsson PM, Baeza A, Palmqvist AEC, Holmberg K (2008) Surfactant inhibition of aluminium pigments for waterborne printing inks. Corr Sci 50:2282–2287
7. Kwon YS, Gromov AA, Ilyin AP, Rim GH (2003) Passivation process for superfine aluminum powders obtained by electrical explosion of wires. Appl Surf Sci 211:57–67
8. Ishihara S, Suematsu H, Nakayama T, Suzuki T, Niihara K (2012) Synthesis of nanosized alumina powders by pulsed wire discharge in air flow atmosphere. Ceram Int 38:4477–4484
9. Mandilas C, Daskalos E, Karagiannakis G, Konstandopoulos AG (2013) Synthesis of aluminium nanoparticles by arc plasma spray under atmospheric pressure. Mater Sci Eng B 178:22–30
10. Mathe VL, Varma V, Raut S, Nandi AK, Pant A, Prasanth H, Pandey RK, Bhoraskar SV, Das AK (2016) Enhanced active aluminum content and thermal behaviour ofnano-aluminum particles passivated during synthesis using thermal plasma route. Appl Surf Sci 368:16–26
11. Lerner MI, Glazkova EA, Lozhkomoev AS, Svarovskaya NV, Bakina OV, Pervikov AV, Psakhie SG (2016) Synthesis of Al nanoparticles and Al/AlN composite nanoparticles by electrical explosion of aluminum wires in argon and nitrogen. Powder Technol 295:307–314
12. Abdelkader EM, Jelliss PA, Buckner SW (2016) Main group nanoparticle synthesis using electrical explosion of wires. Nano-Struct Nano-Obj 7:23–31
13. Yi Z, Xu X, Luo J, Li X, Yi Y, Jiang X, Yi Y, Tang Y (2014) Size controllable synthesis of ultrafine spherical gold particles and their simulation of plasmonic and SERS behaviors. Phys B 438:22–28
14. Huff C, Biehler E, Quach Q, Long JM, Abdel-Fattah TM (2021) Synthesis of highly dispersive platinum nanoparticles and their application in a hydrogen generation reaction. Colloids Surf A 610:125734
15. Liu T, Li D, Yang D, Jiang M (2011) Size controllable synthesis of ultrafine silver particles through a one-step reaction. Mater Lett 65:628–631
16. Nie H, Schoenitz M, Dreizin EL (2012) Calorimetric investigation of the aluminum-water reaction. Int J Hydrog Energy 37:11035–11045
17. Ghanta SR, Muralidharan K (2013) Chemical synthesis of aluminum nanoparticles. J Nanopart Res 15:1715
18. Cui Y, Zhao S, Tao D, Liang Z, Huang D, Xu Z (2014) Synthesis of size-controlled and discrete core-shell aluminum nanoparticles with a wet chemical process. Mater Lett 121:54–57
19. Falola BD, Suni II (2015) Low temperature electrochemical deposition of highly active elements. Curr Opin Solid State Mater Sci 19:77–84
20. Pereira NM, Pereira CM, Araujo JP, Silva AF (2017) Zinc electrodeposition from deep eutectic solvent containing organic additives. J Electroanal Chem 801:545–551
21. Yapontseva YS, Kublanovsky VS, Vyshnevskyi OA (2018) Electrodeposition of CoMoRe alloys from a citrate electrolyte. J Alloys Compd 766:894–901
22. Wang X, Han Y, Zhang J, Li Z, Li T, Zhao X, Liu W (2019) Influence of electropolished copper substrate on morphology of electroplating self-supporting Ni films. Nucl Instrum Meth Phys Res A 927:343–348
23. Lee H, Tsai ST, Wu PH, Dow WP, Chen CM (2019) Influence of additives on electroplated copper films and their solder joints. Mater Charact 147:57–63
24. Shavkunov SP, Strugova TL (2003) Electrode processes during aluminum electrodeposition in aromatic solvents. Russ J Electrochem 39:642–649
25. Jiang T, Chollier Brym MJ, Dubé G, Lasia A, Brisard GM (2007) Studies on the $AlCl_3$/dimethylsulfone ($DMSO_2$) electrolytes for the aluminum deposition processes. Surf Coat Technol 201:6309–6317
26. Yue G, Lu X, Zhu Y, Zhang X, Zhang S (2009) Surface morphology, crystal structure and orientation of aluminium coatings electrodeposited on mild steel in ionic liquid. Chem Eng J 147:79–86
27. Shen Q, Min Q, Shi J, Jiang L, Hou W, Zhu JJ (2011) Synthesis of stabilizer-free gold nanoparticles by pulse sonoelectrochemical method. Ultrason Sonochem 18:231–237
28. Zin V, Pollet BG, Dabalà M (2009) Sonoelectrochemical (20 kHz) production of platinum nanoparticles from aqueous solutions. Electrochim Acta 54:7201–7206
29. Zhu J, Liu S, Palchik O, Koltypin Y, Gedanken A (2000) Shape-controlled synthesis of silver nanoparticles by pulse sonoelectrochemical methods. Langmuir 16:6396–6399
30. Abedin SZE, Moustafa EM, Hempelmann R, Natter H, Endres F (2005) Additive free electrodeposition of nanocrystalline aluminium in a water and air stable ionic liquid. Electrochem Commun 7:1111–1116

31. Mahendiran C, Ganesan R, Gedanken A (2009) Sonoelectrochemical synthesis of metallic aluminum nanoparticles. Eur J Inorg Chem. https://doi.org/10.1002/ejic.200900097
32. Cvetković VS, Vukićević NM, Jovićević N, Stevanović JS, Jovićević JN (2020) Aluminium electrodeposition under novel conditions from $AlCl_3$-urea deep eutectic solvent at room temperature. Trans Nonferrous Met Soc China 30:823–834
33. Liang L, Guo X, Liao X, Chang Z (2020) Improve the interfacial adhesion, corrosion resistance and combustion properties of aluminum powder by modification of nickel and dopamine. Appl Surf Sci 508:144790
34. Rai A, Park K, Zhou L, Zachariah MR (2006) Understanding the mechanism of aluminium nanoparticle oxidation. Combust Theory Model 10:843–859
35. Bard AJ, Faulkner LR (1980) Electrochemical methods: fundamentals and applications. Wiley, New York

Publisher's Note